Published in final edited form as:

Nat Med. 2013 May ; 19(5): 640–645. doi:10.1038/nm.3144.

BAF60c drives glycolytic muscle formation and improves glucose homeostasis through Deptor-mediated AKT activation

Zhuo-Xian Meng[1], **Siming Li**[1], **Lin Wang**[1], **Hwi Jin Ko**[2], **Yongjin Lee**[2], **Dae Young Jung**[2], **Mitsuharu Okutsu**[3], **Zhen Yan**[3], **Jason K. Kim**[2], and **Jiandie D. Lin**[1,*]

[1]Life Sciences Institute and Department of Cell & Developmental Biology, University of Michigan Medical Center, Ann Arbor, MI 48109

[2]Program in Molecular Medicine and Division of Endocrinology, Metabolism and Diabetes, Department of Medicine, University of Massachusetts Medical School, Worcester, MA 01605

[3]Departments of Medicine and Pharmacology, and Center for Skeletal Muscle Research at Robert M. Berne Cardiovascular Research Center, University of Virginia, Charlottesville, VA 22908

Abstract

A shift from oxidative to glycolytic metabolism has been associated with skeletal muscle insulin resistance in type 2 diabetes[1–5]. However, whether this metabolic switch is deleterious or adaptive remains controversial[6–8], in part due to limited understanding of the regulatory network that directs the metabolic and contractile specification of fast-twitch glycolytic muscle. Here we show that BAF60c, a transcriptional cofactor enriched in fast-twitch muscle, promotes a switch from oxidative to glycolytic myofiber type through Deptor-mediated AKT activation. Muscle-specific transgenic expression of BAF60c activates a program of molecular, metabolic, and contractile changes characteristic of glycolytic muscle. In addition, BAF60c is required for maintaining glycolytic capacity in adult skeletal muscle *in vivo*. BAF60c expression is significantly decreased in skeletal muscle from obese mice. Unexpectedly, transgenic activation of the glycolytic muscle program by BAF60c protects mice from diet-induced insulin resistance and glucose intolerance. Further mechanistic studies revealed that Deptor is induced by the BAF60c/Six4 transcriptional complex and mediates activation of AKT and glycolytic metabolism by BAF60c in a cell-autonomous manner. This work defines a fundamental mechanism underlying the specification of fast glycolytic muscle and illustrates that the oxidative to glycolytic metabolic shift in skeletal muscle is potentially adaptive and beneficial in the diabetic state.

*Corresponding Author: Jiandie Lin, Ph.D. 5437 Life Sciences Institute, University of Michigan, 210 Washtenaw Avenue, Ann Arbor, MI 48109, jdlin@umich.edu, Office: (734) 615-3512, Fax: (734) 615-0495.

Note: Supplementary information is available on the Nature Medicine website.

AUTHOR CONTRIBUTIONS

J.D.L. and Z.X.M. conceived the project and designed research. Z.X.M., S.L. and L.W. performed the studies; H.J.K., Y.L., D.Y.J., and J.K.K. performed hyperinsulinemic-euglycemic clamp studies; M.O. and Z.Y. performed muscle fiber typing. Z.X.M. and J.D.L. analyzed the data and wrote the manuscript.

COMPETING FINANCIAL INTERESTS

The authors declare no competing financial interests.

Skeletal myofibers exhibit remarkable diversity and plasticity in energy metabolism and contractile functions. Slow-twitch myofibers are rich in mitochondria and have high oxidative capacity whereas fast-twitch fibers generate ATP primarily through glycolysis[9,10]. The regulatory network that drives the formation of slow-twitch muscle fibers centers on the transcriptional coactivator PGC-1α and its transcriptional partners[10–12]. However, the mechanisms that regulate the specification of fast-twitch glycolytic muscle remain undefined. To identify candidate regulators of glycolytic muscle formation, we analyzed gene expression profiles of soleus and tibialis anterior (TA) (GSE10347)[13], which contain oxidative and mixed myofibers, respectively. This analysis revealed a cluster of transcription factors and cofactors enriched in TA muscle (Fig. 1a), including BAF60c, a subunit of the SWI/SNF chromatin-remodeling complex[14]. BAF60c expression was significantly higher in gastrocnemius, quadriceps, TA, extensor digitorum longus (EDL) and plantaris, muscles enriched for glycolytic fibers, than that of soleus in mice (Fig. 1b). To test whether BAF60c regulates the glycolytic muscle program, we generated muscle-specific BAF60c transgenic (Tg) mice using muscle creatine kinase (MCK) promoter[12]. Two transgenic lines exhibited an approximately 2 to 3-fold increase in BAF60c protein in several muscles (Fig. 1c), which is within its physiological range of expression in different muscles, but not in other tissues, including brown and white adipose tissues, pancreas, heart and liver (data not shown). Skeletal muscle from Tg mice appeared paler in color than that of WT mice. Fiber type analysis indicated that the percentage of type IIa myofiber in plantaris was slightly but significantly decreased in Tg mice, whereas type IIb myofiber content was increased in Tg muscles (Supplementary Fig. 1). Muscle fiber size appeared similar in both groups.

To determine whether BAF60c regulates myofiber energy metabolism, we performed histochemical staining for α-glycerophosphate dehydrogenase (α-GPDH) and succinate dehydrogenase (SDH), which are enriched in glycolytic and oxidative myofibers, respectively[9]. Tg muscles exhibited higher α-GPDH and lower SDH enzymatic activities (Fig. 1d). This shift from oxidative to glycolytic metabolism was observed in all muscles examined, including TA, EDL, and soleus. While intermyofibrillar mitochondria appeared similar, subsarcolemmal mitochondrial content was markedly reduced in Tg myofibers (Fig. 1e). Accordingly, mitochondrial DNA content was lower in Tg muscles (Fig. 1f). The activity of lactate dehydrogenase (LDH) and glycolytic flux were significantly elevated in Tg muscle (Fig. 1g). LDH isoenzyme analysis indicated that the isoenzymes containing LDH-B, which is enriched in oxidative myofibers, were reduced in Tg quadriceps (Supplementary Fig. 2). NADH/NAD^+ ratio was increased, whereas ATP/AMP ratio and AMPK activity were similar. Blood lactate levels were similar between two groups under *ad lib* condition, but remained elevated in the Tg group during starvation. Further, postprandial blood lactate levels following an intraperitoneal injection of 3-mercaptopropionic acid (3-MPA), an inhibitor of PEPCK, were higher in Tg mice. This shift from oxidative to glycolytic metabolism was accompanied by increased glycolytic and reduced oxidative gene expression (Fig. 1h, Supplementary Fig. 2c and 3).

Fast-twitch muscle generates ATP primarily through glycolysis and is more susceptible to exercise-induced fatigue. To determine whether Tg mice have increased glycogen utilization during exercise, we subjected mice to non-exhaustion treadmill running. While basal

glycogen content was similar, transgenic mice exhibited more rapid glycogen depletion during running than control (Supplementary Fig. 4a and Fig. 1i). In a separate study, transgenic mice reached exhaustion significantly earlier than WT control and had shorter total running time and distance (Fig. 1j and data not shown). Post-exercise blood lactate levels were elevated by approximately 50% in BAF60c Tg mice. We conclude from these studies that BAF60c is sufficient to activate a program of molecular, metabolic, and contractile changes characteristic of fast-twitch glycolytic myofibers.

Impaired mitochondrial function has been linked to skeletal muscle insulin resistance. However, whether the shift from oxidative to glycolytic metabolism is deleterious for metabolic homeostasis remains controversial[6–8]. In fact, transgenic activation of mitochondrial oxidative program by PGC-1α is not sufficient to improve skeletal muscle insulin sensitivity in mice[15,16]. Analyses of BAF60c expression revealed that its protein levels were significantly decreased in skeletal muscle from diet-induced and genetic obese mice (Fig. 2a). To determine whether cytokines regulate BAF60c expression, we treated C2C12 myotubes with myostatin (Mstn), interleukin 6 (IL6), or tumor necrosis factor α (TNF-α). As expected, TNF-α induced IL6 expression in myotubes. While Mstn and IL6 had modest effects, TNF-α significantly decreased BAF60c expression in C2C12 and primary human myotubes (Fig. 2b,c). Chromatin-immunoprecipitation (ChIP) assays indicated that TNF-α treatments markedly reduced the levels of acetyl-histone H3 (Ace-H3) and trimethylation of H3 lysine 4 (H3K4m3), epigenetic markers associated with transcriptionally active chromatin, in the proximal BAF60c promoter (Fig. 2d). In contrast, dimethylation of H3 lysine 9 (H3K9m2), a repressive chromatin mark, was augmented in response to TNF-α. These results suggest that BAF60c expression may be repressed in insulin resistant states as a result of epigenetic signaling downstream of proinflammatory cytokines.

To assess the role of glycolytic muscle metabolism in insulin resistance, we subjected WT and Tg mice to high-fat diet (HFD) feeding. Both groups developed obesity with the Tg mice gaining slightly less body weight (Fig. 2e). Compared to control, BAF60c Tg mice had significantly lower fasting blood glucose and insulin levels. The concentrations of plasma lipids, including triglycerides, ketone body, and non-esterified fatty acids (NEFA), were higher in Tg mice (Supplementary Fig. 4b). Insulin tolerance test (ITT) and glucose tolerance test (GTT) indicated that Tg mice were more insulin-sensitive and had improved glucose tolerance (Fig. 2f). Using hyperinsulinemic-euglycemic clamp, we found that glucose infusion rate and whole body glucose turnover were increased in the Tg group. In addition, 2-deoxy-glucose (2-DG) uptake was elevated in Tg gastrocnemius (303 ± 17 nmol g^{-1} min^{-1} for Tg vs. 237 ± 17 nmol g^{-1} min^{-1} for WT; $P < 0.05$). Hepatic glucose production rates were indistinguishable between two groups (Fig. 2g). Skeletal muscle triglyceride content, myokine gene expression, and adipose tissue histology were similar, whereas Tg mice exhibited reduced hepatic steotosis (Fig. 2h and Supplementary Fig. 4c,d). Fatty β-oxidation genes were elevated whereas lipogenic genes were down-regulated in the livers from Tg mice (Supplementary Fig. 5). As such, genetic activation of the glycolytic muscle program protects mice from diet-induced metabolic dysregulation, suggesting that a shift from oxidative to glycolytic phenotype in skeletal myofiber *per se* does not lead to

insulin resistance. Given that resistance training increases glycolytic muscle mass and function and improves metabolic parameters in diabetic patients[25,26], our findings raise the possibility that the oxidative to glycolytic shift may play a previously unappreciated role in skeletal muscle adaptation in type 2 diabetes.

Recent studies demonstrated that conditional AKT activation in muscle is sufficient to enhance glycolytic muscle growth and improve metabolic parameters[17]. Notably, phosphorylation of T308 and S473 residues on AKT was markedly enhanced in Tg quadriceps (Fig. 3a). To identify BAF60c target genes that mediate AKT activation, we compared gene expression profiles of WT and Tg quadriceps and found that Deptor (encoded by *Depdc6*), which was recently identified as an AKT activator and mTOR inhibitor[18], was significantly elevated in Tg muscles (Fig. 3a and Supplementary Fig. 6a,b). Remarkably, Deptor mRNA and protein expression is also highly enriched in glycolytic muscles (Fig. 3b). To establish the cell-autonomous nature of AKT activation by Deptor, we performed gain- and loss-of-function studies in cultured C2C12 myotubes differentiated from transduced myoblasts. Retroviral-mediated overexpression of BAF60c robustly stimulated Deptor mRNA and protein expression and enhanced AKT phosphorylation in cultured myotubes (Fig. 3c and Supplementary Fig. 6c). On the contrary, RNAi knockdown of *BAF60c* resulted in lower Deptor expression and attenuated AKT phosphorylation. These activities of BAF60c are unlikely due to alterations in muscle differentiation (Supplementary Fig. 7). In fact, adenoviral-mediated expression of BAF60c in differentiated C2C12 myotubes also stimulated Deptor expression and AKT phosphorylation. Further, BAF60c dose-dependently stimulated Deptor expression and AKT phosphorylation in cultured primary human myotubes, suggesting that this pathway is conserved between rodents and humans (Fig. 3d).

We next examined the effects of BAF60c on glycolytic metabolism in C2C12 myotubes. Retroviral-mediated BAF60c expression markedly increased, whereas RNAi knockdown decreased the rate of glucose consumption and lactate production (Fig. 3e,f). Glycolytic flux measurements using D-[5-^{3}H]-glucose indicated that BAF60c augmented glycolysis in an AKT-dependent manner (Fig. 3g). Consistently, glycolytic flux was significantly lower in C2C12 myotubes expressing shRNA targeting *BAF60c* (Fig. 3h). Further, BAF60c knockdown attenuated insulin-stimulated AKT activation and glycolytic flux in transduced myotubes (Supplementary Fig. 8a,b). Similar to BAF60c, retroviral-mediated expression of Deptor resulted in a marked increase of AKT phosphorylation, whereas *Deptor* RNAi knockdown had the opposite effects (Supplementary Fig. 8c). To evaluate the role of Deptor in mediating AKT activation by BAF60c, we sequentially transduced C2C12 myoblasts with retroviruses expressing scramble or *Deptor* shRNA followed by a second round of transduction with vector or BAF60c retroviruses. As expected, BAF60c increased Deptor expression and AKT phosphorylation in control myotubes (Fig. 3i). In contrast, RNAi knockdown of *Deptor* nearly abolished the enhancement of AKT phosphorylation by BAF60c. Measurements of lactate production indicated that *Deptor* knockdown severely impaired the ability of BAF60c to increase lactate secretion from transduced myotubes. Taken together, these results demonstrate that the BAF60c/Deptor pathway regulates AKT activation and glycolytic metabolism in myotubes in a cell-autonomous manner.

Recent work has implicated homeobox transcriptional factors Six1 and Six4 in the regulation of fast-twitch muscle genes[19]. Using Genomatix motif analysis, we identified one putative Six4 binding site located 1.6 kb upstream of the transcription start site of the *Deptor* gene. Six4 and BAF60c cooperatively stimulated the expression of endogenous *Deptor* in cultured myotubes and augmented promoter activity via the predicted Six4 binding site (Fig. 4a,b). Chromatin-immunoprecipitation (ChIP) assays revealed that Six4 and BAF60c were recruited to the Six4 binding site through direct physical interaction (Fig. 4c,d). Interestingly, H3K4m3 was markedly increased while H3K9m2 was decreased in proximal *Deptor* promoter in response to BAF60c overexpression (Fig. 4e). These results suggest that BAF60c functions as a coactivator for Six4 and stimulates *Deptor* transcription through altering local chromatin structure and epigenetic landscape.

To evaluate the significance of BAF60c in glycolytic muscle metabolism, we performed *in vivo* RNAi knockdown in skeletal muscle using a mouse strain that transgenically expresses coxsackie adenovirus receptor (MCK-CAR). The efficiency of adenoviral transduction in skeletal myofibers is greatly improved in MCK-CAR mice[20,21]. We injected purified adenoviral vectors expressing *BAF60c* shRNA intramuscularly into TA on one leg and control shRNA on the contralateral leg. Compared to control, *BAF60c* shRNA significantly decreased endogenous BAF60c mRNA and protein expression (Fig. 4f). Accordingly, Deptor mRNA and protein expression was also significantly reduced, suggesting that BAF60c is required for maintaining normal Deptor expression *in vivo*. AKT phosphorylation on both sites was diminished in response to RNAi knockdown of *BAF60c*. To explore whether BAF60c is required for muscle glycolytic metabolism, we performed histochemical staining on transduced muscle. RNAi knockdown of *BAF60c* resulted in increased mitochondrial oxidative capacity (SDH and COX) and decreased α-GPDH staining and LDH activity (Fig. 4g, h). As such, BAF60c is required for maintaining glycolytic myofiber metabolism in adult mice.

The transcriptional program that regulates fast-twitch glycolytic muscle formation remains poorly defined. In this work we delineated a regulatory cascade that drives the metabolic and contractile specification of fast-twitch muscle fibers (Fig. 4i). Both BAF60c and Deptor are enriched in fast glycolytic muscles and cell-autonomously enhance AKT activation. Previous work demonstrated that conditional activation of AKT in skeletal muscle leads to hypertrophic muscle growth[17]. The lack of muscle mass increase in BAF60c Tg mice may be due to relatively modest AKT activation compared to the AKT overexpression model. BAF60c was recently shown to regulate cardiac development and muscle gene expression through transactivating transcription factors including Gata4, Tbx5, Nkx2–5, and MyoD[22,23]. BAF60a, a close homolog of BAF60c, was recently identified as a regulator of hepatic fatty acid β-oxidation[24], raising the possibility that the BAF60 subunit may restrict SWI/SNF-mediated chromatin-remodeling to selective transcriptional targets and elicit specific biological responses.

Genetic and pharmacological manipulations that increase mitochondrial oxidative metabolism have been demonstrated to improve metabolic homeostasis in both humans and rodent models of insulin resistance[11,25–27]. Given the strong association between oxidative myofiber metabolism and insulin sensitivity, why does genetic activation of glycolytic

muscle type ameliorate diet-induced metabolic dysregulation? One possibility is that the shift from oxidative to glycolytic myofiber metabolism may serve as an adaptive response to elevated glucose and insulin in the diabetic state. In fact, resistance training improves metabolic profiles in diabetic patients through promoting the growth and function of fast glycolytic muscle[28,29]. In rodents, inhibition of myostatin signaling leads to glycolytic muscle growth and beneficial effects on glucose homeostasis[30]. Thus, inadequate adaptive increase of skeletal muscle glycolytic capacity may exacerbate insulin resistance, whereas activation of this adaptive mechanism alleviates diet-induced disruption of metabolic homeostasis. Interestingly, BAF60c expression is reduced in skeletal muscle from obese mice as a result of proinflammatory signaling. Our work raises the possibility that expansion of skeletal muscle glycolytic capacity by increasing muscle mass and glycolytic activity, for example through resistance training, may provide metabolic benefits in type 2 diabetes.

ONLINE METHODS

Animal studies

Flag/HA-tagged full-length mouse BAF60c coding sequence (FH-BAF60c) was placed downstream of 4.8 kb murine MCK promoter[31]. Transgenic (Tg) mice were generated by pronuclear microinjection. Six independent founders were identified and crossed with C57BL/6 mice to generate stable Tg lines. For *in vivo* knockdown study, heterozygous MCK-CAR mice were used. Mice were maintained in a 12-h dark and 12-h light cycle and fed with normal rodent chow or high-fat diet (D12492, Research Diets). All animal studies were performed according to procedures approved by the University Committee on Use and Care of Animals. All experiments were performed on male mice unless otherwise indicated.

Histological analysis

Skeletal muscle samples were immediately frozen with liquid nitrogen-cooled isopentane following dissection and sectioned on a cryostat-microtome. Muscle fiber typing immunofluorescence staining was performed with antibodies against MHC I (1:200, DSHB, BA-F8), MHC IIa (1:200, DSHB, SC-71) and MHC IIb (1:200, DSHB, BF-F3), as previously described[32]. SDH and α-GPDH staining was performed as described[33]. COX staining was conducted as previously described[34]. Transmission electron microscopy was performed by Microscopy and Image Analysis Laboratory at University of Michigan. The images were taken using Philips CM-100 transmission electron microscope.

Western blot analysis

Protein lysates were quantified, separated by a SDS-PAGE gel, and transferred to a polyvinylidene difluoride membrane (Millipore), followed by immunoblotted with the following primary antibodies. Rabbit polyclonal antibody against BAF60c was generated with recombinant GST fusion mouse BAF60c protein and affinity purified. Antibodies against Myoglobin (1:1,000, sc-74525), Palvalbumin (1:500, sc-7448), HA (1:1,000, sc-66181), ribosomal protein S6 (1:2,000, sc-74459) were from Santa Cruz. Antibodies against AKT (1:1,000, 4691), phospho-AKT (Ser473) (1:1,000, 4060), phospho-AKT (Thr308) (1:1,000, 2965), p70 S6 kinase (1:1,000, 2708), phospho-p70 S6 kinase (Thr389) (1:1,000, 9234), and phospho-S6 (Ser240/244) (1:1,000, 4838) were from Cell Signaling.

Antibodies against Flag (1:1,000, M2), c-Myc (1:1,000, C3956), and α-tubulin (1:1,000, T6199) were from Sigma. Antibodies to Deptor (1:1,000, 09-463) and BAF53a (1:1,000, 10341-1-AP) were from Millipore and Proteintech, respectively.

Treadmill running

We performed treadmill running studies using a motorized, speed-controlled treadmill system (Columbus Instruments). Running speed was set to 10 m min^{-1} for 30 min and increased by 2 m min^{-1} increments every 20 min. The inclination angle was level. Male mice were trained at a speed of 10 m min^{-1} in three sessions to acquire running skills before running tests. WT and MCK-BAF60c Tg mice were allowed to run until exhaustion for the measurements of total running time and distance. Blood lactate levels were measured prior to the onset of running study and immediately after exhaustion using a Lactate Pro blood lactate test meter (ARKRAY Inc.). In a separate study, Tg mice were subjected to run until exhaustion with running time-matched WT mice used as controls. Mice were anesthetized and skeletal muscles were dissected for the measurement of muscle glycogen content.

In vivo adenoviral transduction in skeletal muscle

Adenoviruses were purified and transduced into TA muscle as previously described[20]. Briefly, MCK-CAR mice were injected intramuscularly into TA with adenoviruses (1×10^8 plaque forming units in 25 μl) expressing scramble shRNA on one leg, and *BAF60c* shRNA on the contralateral leg. The injection was performed twice on two consecutive days. TA muscles were dissected five days following transduction.

ITT and GTT

For GTT, mice were fasted overnight (16 h) and injected intraperitoneally (IP) with a glucose solution (20% prepared in saline) at 2.0 g per kg body weight. Blood glucose concentrations were measured before and 15, 30, 60 and 120 min after glucose injection. For ITT, mice pre-fasted for 4 h were IP injected with insulin at 1.0 U per kg body weight. Blood glucose levels were measured before and 20, 45, 90 and 120 min after insulin injection.

Hyperinsulinemic-euglycemic clamp

We performed hyperinsulinemic-euglycemic clamp study as described[35]. Briefly, a 120-min clamp was conducted with a prime-continuous infusion of human insulin (Humulin; Eli Lilly and Co.) at a rate of 2.5 mU kg^{-1} min^{-1} to raise plasma insulin concentration. Blood samples (20 μl) were collected at 20-min intervals for the immediate measurement of plasma glucose concentration, and 20% glucose was infused at variable rates to maintain plasma glucose at basal concentrations. Insulin-stimulated whole-body glucose turnover and metabolism were estimated using [3-^{3}H] glucose (10 μCi bolus, 0.1 μCi min^{-1}) infusion throughout the clamps. To estimate insulin-stimulated glucose uptake in individual tissues, 2-deoxy-D-[1-^{14}C] glucose (2-[^{14}C] DG; PerkinElmer Inc.) was administered as a bolus (10 μCi) at 75 min after the start of the clamps. Blood samples (20 μl) were taken at 80, 85, 90, 100, 110, and 120 min after the start of the clamps for the determination of plasma [^{3}H]

glucose, $^{3}H_2O$, and 2-[^{14}C] DG concentrations. At the end of the clamp experiments, mice were anesthetized and tissues were harvested for biochemical analysis.

Muscle cell culture, retroviral infection and differentiation

C2C12 myoblasts were obtained from ATCC and cultured in DMEM containing 10% fetal bovine serum. Pooled primary human skeletal myoblasts isolated from three healthy adult donors were purchased from Zen-Bio and maintained in skeletal muscle growth medium (SKM-M, Zen-Bio). Myoblasts were transduced with control retroviruses (vector or scramble shRNA control) or retroviruses expressing BAF60c, Deptor, Six4 or shRNAs targeting *BAF60c* or *Deptor*, and subjected to puromycin selection. For sequential retroviral transduction, myoblasts stably transduced with scramble or *Deptor* shRNA retroviruses were transduced again with retroviruses expressing vector control or BAF60c followed by neomycin selection. Myotube differentiation was initiated by switching confluent C2C12 or primary human myoblasts to DMEM containing 2% bovine growth serum or skeletal muscle differentiation medium (SKM-D, Zen-Bio), respectively. All studies were performed in differentiated myotubes.

CoIP and ChIP

293T cells were transiently transfected with FH-Six4 and Myc-tagged BAF60c for 24 h. Total lysates or immunoprecipitated proteins were analyzed by western blot using monoclonal antibodies against c-Myc (Sigma, C3956) or Flag (Sigma, M2). Chromatin immunoprecipitation (ChIP) assay was performed according to the protocol developed by Upstate Biotechnology as described[24]. Briefly, chromatin lysates were prepared from C2C12 myotubes following crosslinking with 1% formaldehyde. The samples were pre-cleared with Protein-G agarose beads and immunoprecipitated using antibodies against BAF60c (as described above), Six4 (Santa Cruz, sc-55766), Acetyl-H3 (Upstate, 06-599), H3K4m3 (Upstate, 07-473), H3K9m2 (Abcam, ab1220), or control IgG in the presence of BSA and salmon sperm DNA. Beads were extensively washed before reverse crosslinking. DNA was purified using a PCR Purification Kit (Invitrogen) and subsequently analyzed by qPCR using primers located in the proximal *BAF60c* or *Deptor* promoter (Primers in Supplementary Table 1).

Luciferase reporter assay

The proximal *Deptor* promoter (−2258 to +23 relative to transcriptional start site) was cloned into pGL3 luciferase reporter vector. Six4 binding site mutant was constructed by site-directed mutagenesis. C2C12 myoblasts were transiently transfected with indicated plasmids using Lipofectamine 2,000 and differentiated into myotubes prior to luciferase assay. All the reporter assays were repeated at least three times in triplicates.

LDH activity assay and isoenzyme analysis

Skeletal muscle LDH activity was measured using an assay kit (BioVision). Briefly, frozen muscle tissue was homogenized in 0.25 ml cold assay buffer. Following centrifugation at 10,000 g for 15 min at 4 °C, the supernatant was collected for the enzymatic assay. The activities of LDH isoenzymes were determined as previously described[36]. Briefly, whole

cell lysates of plantaris muscles were loaded on a 6% native polyacrylamide gel. Following electrophoresis, the gel was stained at room temperature for 30 min.

Measurement of glycolytic flux

The rate of glycolysis in isolated skeletal muscles and cultured myotubes were measured using D-[5-^{3}H]-glucose (American Radiolabeled Chemicals) as previously described[37] with some modifications. Briefly, EDL muscles dissected from WT and Tg male mice, or cultured myotubes were incubated for 1 h at 37 °C in Krebs buffer with 10 μCi ml^{-1} D-[5-^{3}H]-glucose plus 5 mM glucose for isolated muscles or 10 mM glucose for myotubes. ^3H_2O produced by glycolysis was separated from D-[5-^{3}H]-glucose in the incubation buffer using equilibration method[38] and determined by liquid scintillation counting.

Statistics

Data were analysed using two-tailed Student's *t*-test for independent groups. A P value of less than 0.05 was considered statistically significant.

Supplementary Material

Refer to Web version on PubMed Central for supplementary material.

ACKNOWLEDGEMENTS

We are grateful to S. Gu and C. Rui for assistance in experiments and lab members for discussion. We thank J. Nalbantoglu and P. C. Holland (McGill University) for the generous gift of MCK-CAR transgenic mouse strain. We thank the staff at the University of Michigan Transgenic Animal Core for the generation of MCK-BAF60c Tg mice, D. Sorenson for help with EM study, and support from Michigan Diabetes Research and Training Center (DK020572) and Nutrition Obesity Research Center (DK089503). This work was supported by NIH (DK095151 and DK077086, J.D. Lin). Z.X. Meng and S. Li are supported by Postdoctoral Fellowship and Scientist Development Grant from American Heart Association, respectively. Clamp studies were performed at the UMass Mouse Metabolic Phenotyping Center and supported by NIH (U24-DK093000 and R01-DK080756, J.K. Kim). M. Okutsu and Z. Yan are supported by NIH (AR050429).

References

1. Kelley DE, He J, Menshikova EV, Ritov VB. Dysfunction of mitochondria in human skeletal muscle in type 2 diabetes. Diabetes. 2002; 51:2944–2950. [PubMed: 12351431]
2. Lillioja S, et al. Skeletal muscle capillary density and fiber type are possible determinants of *in vivo* insulin resistance in man. J Clin Invest. 1987; 80:415–424. [PubMed: 3301899]
3. Mootha VK, et al. PGC-1alpha-responsive genes involved in oxidative phosphorylation are coordinately downregulated in human diabetes. Nat Genet. 2003; 34:267–273. [PubMed: 12808457]
4. Patti ME, et al. Coordinated reduction of genes of oxidative metabolism in humans with insulin resistance and diabetes: Potential role of PGC1 and NRF1. Proc Natl Acad Sci U S A. 2003; 100:8466–8471. [PubMed: 12832613]
5. Petersen KF, Dufour S, Befroy D, Garcia R, Shulman GI. Impaired mitochondrial activity in the insulin-resistant offspring of patients with type 2 diabetes. The New England journal of medicine. 2004; 350:664–671. [PubMed: 14960743]
6. Muoio DM. Intramuscular triacylglycerol and insulin resistance: guilty as charged or wrongly accused? Biochim Biophys Acta. 2010; 1801:281–288. [PubMed: 19958841]
7. Turner N, Heilbronn LK. Is mitochondrial dysfunction a cause of insulin resistance? Trends Endocrinol Metab. 2008; 19:324–330. [PubMed: 18804383]

8. Muoio, Deborah M.; Neufer, PD. Lipid-Induced Mitochondrial Stress and Insulin Action in Muscle. Cell metabolism. 2012; 15:595–605. [PubMed: 22560212]
9. Schiaffino S, Reggiani C. Fiber types in mammalian skeletal muscles. Physiol Rev. 2011; 91:1447–1531. [PubMed: 22013216]
10. Bassel-Duby R, Olson EN. Signaling pathways in skeletal muscle remodeling. Annual review of biochemistry. 2006; 75:19–37.
11. Lagouge M, et al. Resveratrol improves mitochondrial function and protects against metabolic disease by activating SIRT1 and PGC-1alpha. Cell. 2006; 127:1109–1122. [PubMed: 17112576]
12. Lin J, et al. Transcriptional co-activator PGC-1 alpha drives the formation of slow-twitch muscle fibres. Nature. 2002; 418:797–801. [PubMed: 12181572]
13. Lavery GG, et al. Deletion of hexose-6-phosphate dehydrogenase activates the unfolded protein response pathway and induces skeletal myopathy. J Biol Chem. 2008; 283:8453–8461. [PubMed: 18222920]
14. Wu JI, Lessard J, Crabtree GR. Understanding the words of chromatin regulation. Cell. 2009; 136:200–206. [PubMed: 19167321]
15. Choi CS, et al. Paradoxical effects of increased expression of PGC-1alpha on muscle mitochondrial function and insulin-stimulated muscle glucose metabolism. Proc Natl Acad Sci U S A. 2008; 105:19926–19931. [PubMed: 19066218]
16. Miura S, Kai Y, Ono M, Ezaki O. Overexpression of peroxisome proliferator-activated receptor gamma coactivator-1alpha down-regulates GLUT4 mRNA in skeletal muscles. J Biol Chem. 2003; 278:31385–31390. [PubMed: 12777397]
17. Izumiya Y, et al. Fast/Glycolytic muscle fiber growth reduces fat mass and improves metabolic parameters in obese mice. Cell Metab. 2008; 7:159–172. [PubMed: 18249175]
18. Peterson TR, et al. DEPTOR is an mTOR inhibitor frequently overexpressed in multiple myeloma cells and required for their survival. Cell. 2009; 137:873–886. [PubMed: 19446321]
19. Niro C, et al. Six1 and Six4 gene expression is necessary to activate the fast-type muscle gene program in the mouse primary myotome. Dev Biol. 2010; 338:168–182. [PubMed: 19962975]
20. Civitarese AE, et al. Regulation of skeletal muscle oxidative capacity and insulin signaling by the mitochondrial rhomboid protease PARL. Cell Metab. 2010; 11:412–426. [PubMed: 20444421]
21. Nalbantoglu J, et al. Muscle-specific overexpression of the adenovirus primary receptor CAR overcomes low efficiency of gene transfer to mature skeletal muscle. J Virol. 2001; 75:4276–4282. [PubMed: 11287577]
22. Forcales SV, et al. Signal-dependent incorporation of MyoD-BAF60c into Brg1-based SWI/SNF chromatin-remodelling complex. Embo J. 2011; 31:301–316. [PubMed: 22068056]
23. Lickert H, et al. Baf60c is essential for function of BAF chromatin remodelling complexes in heart development. Nature. 2004; 432:107–112. [PubMed: 15525990]
24. Li S, et al. Genome-wide coactivation analysis of PGC-1alpha identifies BAF60a as a regulator of hepatic lipid metabolism. Cell Metab. 2008; 8:105–117. [PubMed: 18680712]
25. Banks AS, et al. SirT1 gain of function increases energy efficiency and prevents diabetes in mice. Cell Metab. 2008; 8:333–341. [PubMed: 18840364]
26. Narkar VA, et al. AMPK and PPARdelta agonists are exercise mimetics. Cell. 2008; 134:405–415. [PubMed: 18674809]
27. Timmers S, et al. Calorie restriction-like effects of 30 days of resveratrol supplementation on energy metabolism and metabolic profile in obese humans. Cell Metab. 2011; 14:612–622. [PubMed: 22055504]
28. Gordon BA, Benson AC, Bird SR, Fraser SF. Resistance training improves metabolic health in type 2 diabetes: a systematic review. Diabetes Res Clin Pract. 2009; 83:157–175. [PubMed: 19135754]
29. LeBrasseur NK, Walsh K, Arany Z. Metabolic benefits of resistance training and fast glycolytic skeletal muscle. Am J Physiol Endocrinol Metab. 2011; 300:E3–E10. [PubMed: 21045171]
30. Akpan I, et al. The effects of a soluble activin type IIB receptor on obesity and insulin sensitivity. Int J Obes (Lond). 2009; 33:1265–1273. [PubMed: 19668253]

31. Sternberg EA, et al. Identification of upstream and intragenic regulatory elements that confer cell-type-restricted and differentiation-specific expression on the muscle creatine kinase gene. Mol Cell Biol. 1988; 8:2896–2909. [PubMed: 3405222]

32. Waters RE, Rotevatn S, Li P, Annex BH, Yan Z. Voluntary running induces fiber type-specific angiogenesis in mouse skeletal muscle. Am J Physiol Cell Physiol. 2004; 287:C1342–C1348. [PubMed: 15253894]

33. Dunn SE, Michel RN. Coordinated expression of myosin heavy chain isoforms and metabolic enzymes within overloaded rat muscle fibers. Am J Physiol. 1997; 273:C371–C383. [PubMed: 9277335]

34. Zechner C, et al. Total skeletal muscle PGC-1 deficiency uncouples mitochondrial derangements from fiber type determination and insulin sensitivity. Cell Metab. 2010; 12:633–642. [PubMed: 21109195]

35. Kim JK, et al. PKC-theta knockout mice are protected from fat-induced insulin resistance. J Clin Invest. 2004; 114:823–827. [PubMed: 15372106]

36. Gan Z, et al. The nuclear receptor PPARbeta/delta programs muscle glucose metabolism in cooperation with AMPK and MEF2. Genes Dev. 2011; 25:2619–2630. [PubMed: 22135324]

37. Aragones J, et al. Deficiency or inhibition of oxygen sensor Phd1 induces hypoxia tolerance by reprogramming basal metabolism. Nat Genet. 2008; 40:170–180. [PubMed: 18176562]

38. Hughes SD, Quaade C, Johnson JH, Ferber S, Newgard CB. Transfection of AtT-20ins cells with GLUT-2 but not GLUT-1 confers glucose-stimulated insulin secretion. Relationship to glucose metabolism. J Biol Chem. 1993; 268:15205–15212. [PubMed: 8325893]

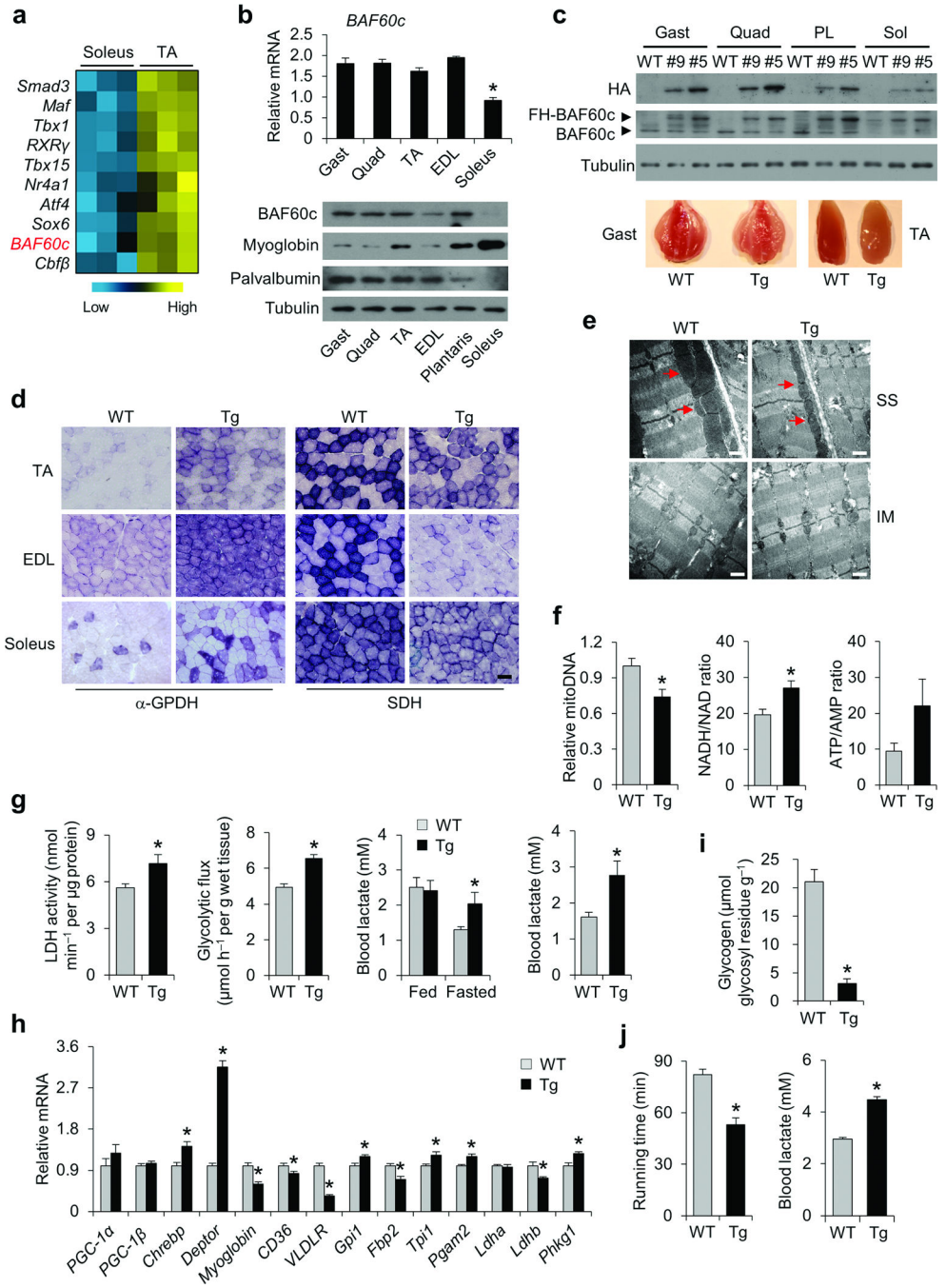

Figure 1. BAF60c promotes fast-twitch glycolytic muscle formation

(**a**) Clustering analysis of transcription factor/cofactor expression in soleus and tibialis anterior (TA) muscles. (**b**) Top, qPCR analysis of *BAF60c* mRNA expression in indicated muscles (n = 3); Bottom, immunoblots of total muscle protein lysates. Gast, gastrocnemius; Quad, quadriceps; EDL, extensor digitorum longus. (**c**) Top, immunoblots of total muscle protein lysates; Bottom, appearance of skeletal muscles from WT and Tg mice. (**d**) Representative histochemical staining of α-GPDH (left) and SDH (right) enzymatic activity (n = 6). Scale bar, 100 μm. (**e**) Transmission electron micrographs of TA muscle. Arrows

point to subsarcolemmal mitochondria. SS, subsarcolemmal; IM, intermyofibrillar. Scale bars, 500 nm. (**f**) Left, relative mitochondrial DNA content in plantaris; Middle and Right, NADH/NAD and ATP/AMP ratio. (**g**) Left, LDH activity in plantaris (n = 7–9); Middle, glycolytic flux in isolated EDL muscle (n = 10); Right, blood lactate levels under fed and fasted (n = 7–9) or postprandial (n = 6–9) states. (**h**) qPCR analysis of gene expression in plantaris muscle (n = 7–8). (**i**) TA muscle glycogen content in running time-matched mice (n = 6). (**j**) Running time and blood lactate levels in WT and Tg mice at exhaustion (n = 6). Values are mean ± s.e.m.; *P < 0.05 by two-tailed Student's t-test.

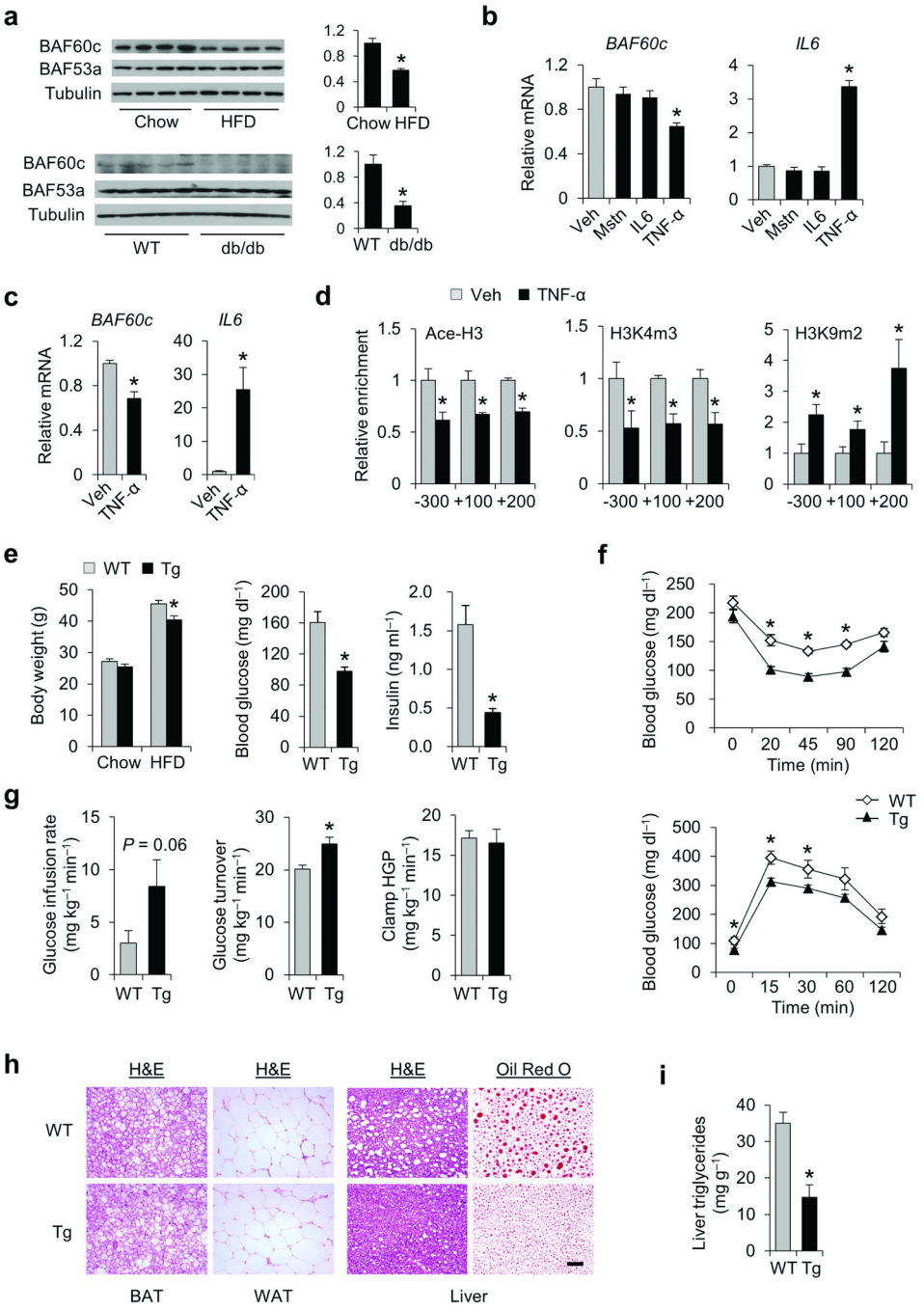

Figure 2. BAF60c transgenic mice are protected from diet-induced insulin resistance

(**a**) Left, immunoblots of total protein lysates from quadriceps muscle. Right, quantitation of BAF60c protein levels after normalization to α-tubulin. (**b,c**) qPCR analysis of gene expression in differentiated C2C12 myotubes (**b**) and primary human myotubes (**c**) treated with vehicle (Veh) or indicated cytokines. (**d**) ChIP assays in C2C12 myotubes treated with vehicle or TNF-α for 3 h. (**e**) Left, body weight of male mice fed with chow or high-fat diet (HFD) for 12 weeks (n = 14–15); Middle and Right, fasting blood glucose and plasma insulin levels in mice fed with HFD for 12-weeks (n = 8–9). (**f**), insulin tolerance test (top),

and glucose tolerance test (bottom) in mice fed with HFD for 12-weeks (n = 8–9). (**g**) Clamp glucose infusion rate, whole body glucose turnover, and hepatic glucose production (HGP) rate measured by hyperinsulinemic-euglycemic clamp in HFD-fed mice (n = 11–12). (**h**) Histology of metabolic tissues and Oil Red O staining of liver sections. Scale bar, 100 μm. (**i**) Liver triglyceride content (n = 8–9). For **b–d**, values are mean ± s.d. and are representative of three independent experiments. For **a, e–g** and **i**, data are mean ± s.e.m.; *P < 0.05 by two-tailed Student's t-test.

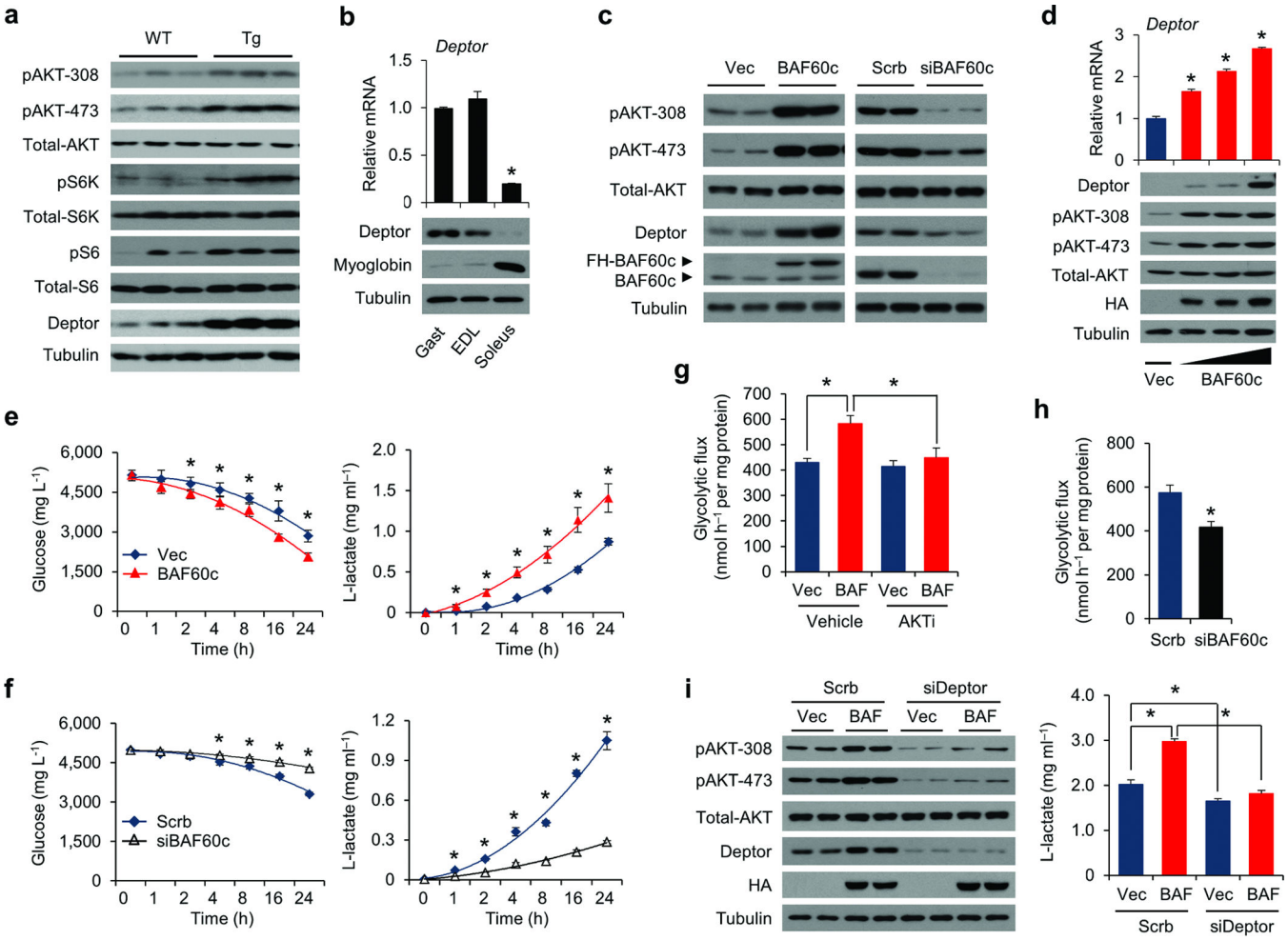

Figure 3. BAF60c activates AKT pathway through Deptor in a cell-autonomous manner

(**a**) Immunoblots of total protein lysates from WT and Tg quadriceps. (**b**) Deptor mRNA and protein expression in indicated muscles. Values are mean ± s.e.m.; **P* < 0.05 by two-tailed Student's *t*-test, soleus vs. other muscles. (**c**) Immunoblots of total lysates from transduced C2C12 myotubes. (**d**) qPCR analysis of *Deptor* mRNA and immunoblots of total lysates from transduced primary human myotubes. (**e,f**) Glucose and lactate concentrations in culture media from transduced C2C12 myotubes. (**g**) Glycolytic flux in transduced C2C12 myotubes treated with vehicle or 10 μM of AKT1/2 inhibitor (AKTi) for 1 h. (**h**) Glycolytic flux in transduced C2C12 myotubes under basal condition. (**i**) Left, immunoblots of protein lysates from transduced C2C12 myotubes. Right, lactate concentrations in culture media from transduced C2C12 myotubes. For **d–I**, Data represent mean ± s.d. and are representative of three independent experiments; **P* < 0.01 by two-tailed Student's *t*-test. FH-BAF60c, Flag/HA-tagged-BAF60c; Vec, Vector; BAF, BAF60c; Scrb, Scramble.

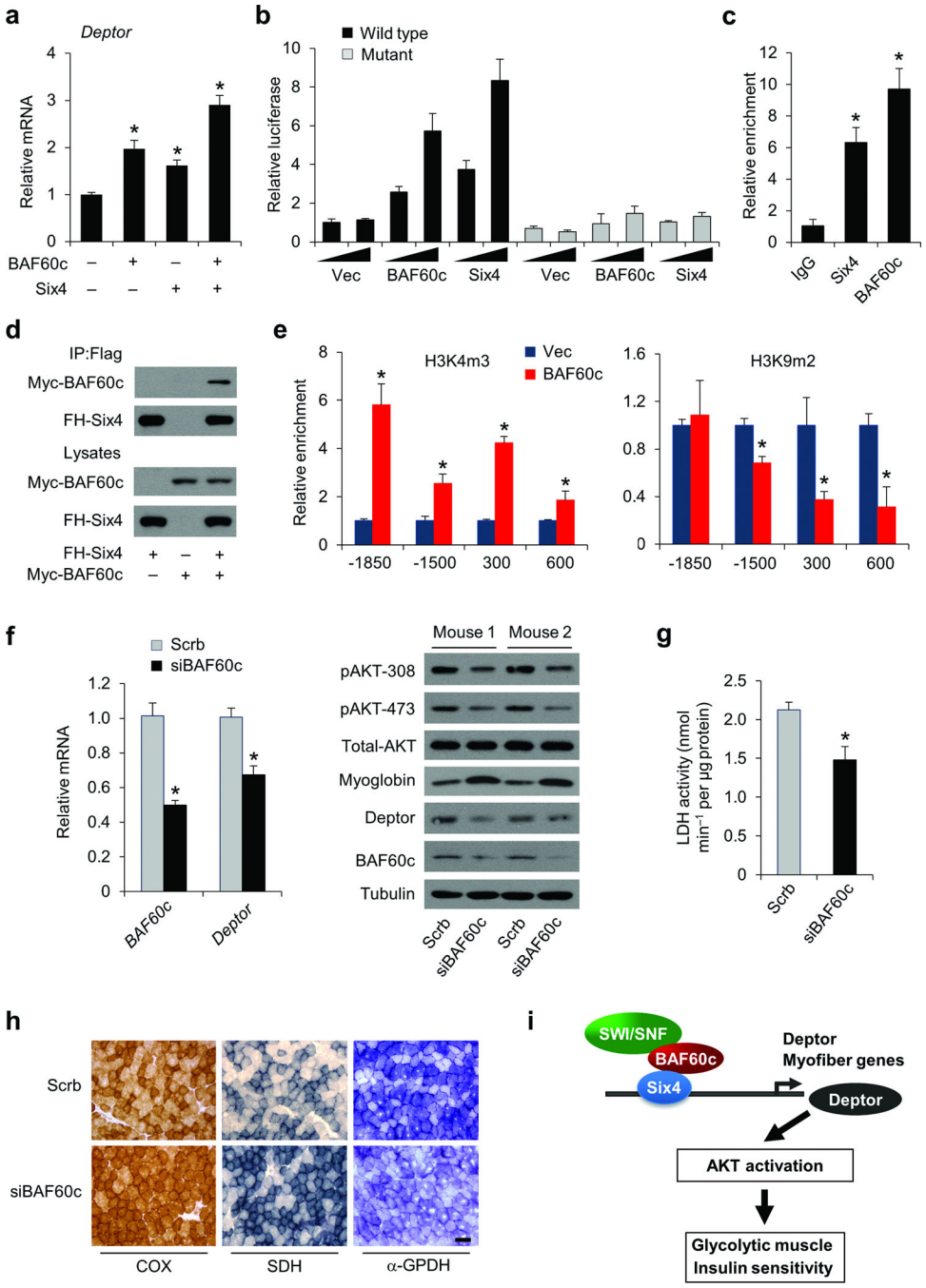

Figure 4. BAF60c is required for maintaining glycolytic metabolism in adult skeletal muscle

(**a**) *Deptor* mRNA expression in C2C12 myotubes transduced with indicated adenoviral vectors. (**b**) Reporter gene assay with constructs containing wild type or Six4 binding site mutated *Deptor* promoter. (**c**) Relative enrichment of BAF60c and Six4 on putative Six4 binding site on proximal *Deptor* promoter. (**d**) Physical interaction of Six4 and BAF60c in transiently transfected 293T cells. (**e**) ChIP assay in transduced myotubes using anti-H3K4m3 and H3K9m2 antibodies. The locations of qPCR primers are relative to the transcriptional start site of *Deptor* gene. (**f**) Left, *BAF60c* and *Deptor* mRNA levels in TA

muscle transduced with indicated adenoviral vectors (n = 6); Right, immunoblots of total protein lysates from transduced TA muscle. Shown are representative blots of two mice. (**g**) LDH enzymatic activity in transduced TA (n = 8). (**h**) Representative histochemical staining of COX (left), SDH (middle), and α-GPDH (right) activities on frozen sections of transduced TA muscle (n = 8). (**i**) Model depicting the BAF60c/Deptor/AKT regulatory cascade in metabolic and contractile specification of fast-twitch glycolytic muscle. Data in **a–c**, and **e** represent mean ± s.d. and are representative of three independent experiments; Data in **f** and **g** represent mean ± s.e.m.; *P < 0.01 by two-tailed Student's t-test.